Frontiers in Health InformaticsISSN-Online: 2676-7104 www.healthinformaticsjournal.com
2024; Vol 13: Issue 3 Open Access

Formulation And Evaluation Of Zinc Oxide Nanocarriers For Antibacterial Activity

Jayendra Kumar [1], Nagegowda P [2], Maheshwar Gurunath Hogade [3], D.Chinababu [4], Deepti Dwivedi [5], Ankur Srivastava [6],Vijay Prakash [7], Mahesh Kumar Posa [8]*

1. Professor, Professor & Principal, SRM Modinagar College of Pharmacy, SRM Institute of Science and Technology, Delhi-NCR Campus, Ghaziabad, Uttar Pradesh, 201204
2. Associate Professor, Government First Grade College, Channapatna 562160
3. Principal, MAEER Pune's, Maharashtra Institute of Pharmaceutical Sciences, Latur, Vishwanathpuram, Ambajogai Road, Latur-413531
4. Professor, Institute of Pharmaceutical Sciences and Research for Girls, Swami Chincholi, Bhigwan, Pune, Maharashtra, Pin-413130
5. Assistant Professor, Institute of Pharmacy- Dr Shakuntala Misra National Rehabilitation University 226022
6. Assistant Professor, Institute of Pharmacy, Dr Rammanohar Lohia Avadh University, Ayodhya, Pin Code-224001
7. Assistant Professor, L R Institute of Pharmacy, Solan HP 173223
8. Associate Professor, Department of Pharmacology, School of Pharmaceutical Sciences, Jaipur National University, Jagatpura, Jaipur- 302017

Corresponding Author: Dr. Mahesh Kumar Posa
Designation and Affiliation: Associate Professor, Department of Pharmacology, School of Pharmaceutical Sciences, Jaipur National University, Jagatpura, Jaipur- 302017
Email id: posa.mahesh@gmail.com

Cite this paper as: Jayendra Kumar , Nagegowda P , Maheshwar Gurunath Hogade , D.Chinababu, Deepti Dwivedi , Ankur Srivastava ,Vijay Prakash , Mahesh Kumar Posa (2024) Formulation And Evaluation Of Zinc Oxide Nanocarriers For Antibacterial Activity . *Frontiers in Health Informatics, 13* (3), 5470-5478

ABSTRACT: Zinc oxide nanoparticles were synthesised via polyol-mediated synthesis in this study. Refluxing zinc acetate precursor in diethylene glycol (DEG) and triethylene glycol (TEG) with and without sodium acetate for two and three hours was how the synthesis process was completed. To characterise the antibacterial activity of produced ZnO nanoparticles (ZF1-ZF8) against various bacteria, including Salmonella typhi, Escherichia coli, Bacillus subtilis, Klebsiella pneumoniae, Pseudomonas aeruginosa, and Staphylococcus aureus. X-ray diffraction (XRD), UV visible spectroscopy (UV), thermogravimetric analysis (TGA), Fourier Transform Infrared Spectroscopy (FTIR), scanning electron microscopy (SEM), and transmission electron microscopy (TEM) were used to characterise all of the synthesised ZnO nanoparticles (ZF1-ZF8). Using the agar-well diffusion method, an antibacterial investigation was conducted on both gram-positive and gram-negative bacterial strains. While ZF7 and ZF8 demonstrated higher activity on some strains than others, ZF3 exhibited nearly constant activity on all of the strains. According to the results, ZnO nanoparticles may find use as antibacterial agents; however, the way in which they work depends on surface changes and composition.

KEYWORDS: Zinc Oxide nanoparticles, Synthesis, XRD, antibacterial study, agar diffusion method.

INTRODUCTION

The "gold standard" for treating many bacterial illnesses nowadays is the use of antibiotics [1, 2]. Microorganisms may, nevertheless, grow resistant to antibiotics. Most pathogenic bacteria are capable of

becoming resistant to at least some antimicrobial agents [3]. Numerous mechanisms, including drug penetration inhibition [4, 5], antibiotic target modifications [6, 7], antibiotic enzymatic inactivation [8], active antibiotic excretion from a cell [4], and others, contribute to the development of antibiotic resistance in bacteria.

Lower respiratory infections and gastrointestinal illnesses rank among the top 10 determinants of morbidity and mortality, according to data from the World Health Organisation (WHO) [9]. The emergence of strains resistant to antibiotics dramatically raised the death toll and intensity of bacterial infections. Globally, the number of deaths from diabetes and cancer is less than the overall number of deaths from antibiotic-resistant bacterial strains [10, 11]. Antibiotic resistance has been confirmed against nearly all of the current antibiotics, despite their substantial quantities. Shortly after a novel medication is licensed for usage, antibiotic resistance develops [3, 12]. The WHO was asked to support the global action plan on antibiotic resistance in 2021 by the events listed [13]. The aforementioned factors make the global public health community's quest for novel antimicrobial preparations a top priority. Since ancient times, people have utilised the antibacterial qualities of certain metals and their ions. It is known today that a wide range of metals has the antimicrobial activity: Ag, Al, As, Cd, Co, Cr, Cu, Fe, Ga, Ni, Pb, Sb, Te, Zn [14].

The ability of metal ions to inhibit enzymes, promote the production of reactive oxygen species (the Fenton reaction) [15–16], damage cell membranes [16–17], and prevent microbes from absorbing essential microelements [18] forms the basis of metals' antimicrobial activity. Moreover, some metals can directly cause genotoxicity. There is a lot of interest in using metal-based nanoparticles and their oxides. Zinc (Zn) and its oxide are among the well-researched metals that have an impact on biological things (ZnO). Strong reduction properties are exhibited by zinc, making it an active element. Zinc oxide can be easily formed by oxidising it. Being one of the most significant trace elements, zinc has a significant function in the human body [19]. All bodily tissues contain zinc, however myocytes contain the largest concentration of zinc (85% of the body's total zinc level) [20]. Zinc has both a structural and catalytic role in several macromolecules and enzymes, where it has been demonstrated to be essential for their correct operation. Conversely, zinc finger architectures offer a special framework that enables interactions between protein subdomains and other proteins or DNA [21]. When many metal oxide nanoparticles come into contact with bacteria, ROS are produced [22]. Certain enzymes are inhibited and the respiratory chain is impacted by the metal ions that the nanoparticles release. Singlet oxygen, hydroxyl radicals, hydrogen peroxide, superoxide anions, and other ROS are produced as a result and accumulate. ROS have the ability to harm DNA and proteins, which are internal bacterial components [23].

In the current study, ZnO nanoparticles were created using three distinct methods: (i) routine synthesis in polyols; (ii) in the presence of sodium acetate; and (iii) lengthening the reaction time. Different approaches have been used by us to create ZnO nanoparticles. The primary step in the synthesis process is the refluX of zinc acetate dihydrate precursor in diethylene glycol (DEG) and triethylene glycol (TEG), both with and without sodium acetate, a weak base, during a range of reaction times. [24] The impact of these two polyols, reaction time, and the presence or absence of sodium acetate on size. [25] These nanoparticles were studied for their antibacterials activity against *Bacillus subtilis, Escherichia coli, Klebsiella pneumoniae, Pseudomonas aeruginosa, Salmonella typhi and Staphylococcus aureus.*

MATERIALS AND METHODS:

Materials: All chemicals used here were of analytical grade and used without further purification. All chemicals were purchased from S.D fine chemicals, Mumbai, India. The media have been procured from Himedia Laboratories Pvt. Ltd, Mumbai, India. Distilled water was used in the all experiments.

Synthesis of ZnO nanoparticles: Precursor zinc acetate dihydrate (0.1 M) was refluxed in diethylene glycol and triethylene glycol at 180 and 220 degrees Celsius, respectively, to create ZnO nanoparticles. With and without sodium acetate (0.01 M), the reaction time varied between two and three hours. The solution was stirred for 1.5 hours at 80°C on a magnetic stirrer before refluxing. Following the reflux action, the samples were

centrifuged for 15 minutes at 8000 rpm and then three times in distilled water and ethanol. Additionally, it was dried for an entire night at 80°C (Table 1). [26] First, esterification results from the interaction of zinc acetate dihydrate with DEG/TEG, forming $(Zn\text{-}OH)_2$. As (Zn-OH)2 is further dehydrated, ZnO nanoparticles are formed. [27] The fundamental method for adding sodium acetate involved adding extra acetate ions, which resulted in distinct particle morphologies from those produced when sodium acetate was not present. The release rate of OH^- is regulated by a mild hydrolysation that is brought on by sodium acetate.

Table 1: Reaction conditions used for synthesis of Zinc oxide nanoparticles

F. Code	Glycol used	Zinc acetate dihydrate	Sodium acetate	Hydration ratio	Reaction time and temperature
ZF1	Diethylene glycol	0.1 M	-	2h	2 h at 180 °C
ZF2	Diethylene glycol	0.1 M	0.01 M	2h	2 h at 180 °C
ZF3	Diethylene glycol	0.1 M	-	2h	3 h at 180 °C
ZF4	Diethylene glycol	0.1 M	0.01 M	2h	3 h at 180 °C
ZF5	Triethylene glycol	0.1 M	-	2h	2 h at 220 °C
ZF6	Triethylene glycol	0.1 M	0.01 M	2h	2 h at 220 °C
ZF7	Triethylene glycol	0.1 M	-	2h	3 h at 180 °C
ZF8	Triethylene glycol	0.1 M	0.01 M	2h	3 h at 180 °C

Characterization: Using r-Ray Diffraction, ZnO nanoparticles were characterised to identify the chemical and ascertain its crystalline shape. Using a Rigaku 600Miniflex X-ray diffraction equipment (XRD) with Cukα radiation (λ = 1.5412 Å) in the scanning range of 100-800, X-ray diffraction studies of ZnO NPs were conducted. Agilent Technologies Cary 60 UV-vis was used to carry out UV–visible (UV–vis) spectra in the wavelength range of 200–600 nm in order to verify the absorbance of ZnO NPs and to track changes in the absorbance brought on by variations in reaction circumstances. To determine which distinctive functional groups are present on the ZnO surface, All samples' Fourier transform infrared (FTIR) spectra were captured in the 400–4000 cm^{-1} range using JASCO INC 410, Japan. Using the PerkinElmer STA-5000 equipment, thermal gravimetric analysis (TGA) was used to monitor the thermal stability of zinc oxide. Every sample was heated at a rate of 10 °C per minute, from 50 to 900 °C. Transmission electron microscopy (TEM) and scanning electron microscopy (SEM) were used to examine the surface morphology of all synthesised ZnO. [28-30]

Evaluation of antimicrobial activity of Zinc Oxide nanoparticles Antibacterial study: Using Luria Bertani growth media, the antibacterial activity of zinc oxide nanoparticles was assessed using the agar-well diffusion method [31]. Clinical isolates of Salmonella typhi, Escherichia coli, Pseudomonas aeruginosa, Bacillus subtilis, and Staphylococcus aureus were used to investigate the antibacterial activity. After preparing the luria-bertani broth, the pH was adjusted to 7.2–7.5 and it was autoclaved. Test tubes filled with the cooked broth were used. Separate inoculations of each strain were made into culture broth. In a shaker incubator, the culture test tubes were incubated at 37°C for the entire night. [32]

Plating: After making the luria-Bertani agar, 25 millilitres of it were added to each petriplate and left to solidify. Pipetting 50µl of Bacillus subtilis cell suspension onto an agar plate was done. To guarantee that the culture was distributed uniformly, a cotton swab was used to thoroughly swab the culture. Using gel puncture, 5 wells were created on the agar, with enough space between them. Samples of varying concentrations were placed into the designated wells after they were labelled. The remaining five strains underwent the same process. The plates were incubated in the incubator at 37°C for 16 to 18 hours. [33] The bacteria's zone of inhibition was measured around each well, and the results were recorded in millimetres (mm). The values were subject to analysis using ANOVA software to determine the mean values and standard error. [34]

RESULTS AND DISCUSSION

X-ray diffraction studies: ZnO nanoparticle diffractograms are shown in Figures 1 and 2. JCPDS Card No. 36-1451 is in agreement with the XRD results of all samples with 2θ values and reflection planes at 31.72° (100), 34.39° (002), 36.23° (101), and 47.44° (102). Therefore, all of the diffraction peaks match the hexagonal wurtzite structure of ZnO well, demonstrating the efficacy of the polyol hydrolysis process in producing ZnO.

Elemental Analysis: Using EDX spectroscopy, the elemental composition of every ZnO nanostructure was examined. The synthesis of pure ZnO nanoparticles is shown by the presence of Zn and O in the EDX of all synthesised ZnO nanoparticles. The antimicrobial and antibiofilm action of the impurity-free nanoparticle seems promising.

UV Spectra of ZnO nanoparticles: UV absorption spectroscopy was used to characterise the optical characteristics of ZnO nanoparticles. The ZnO nanoparticles' UV–vis absorption curves were displayed after they were calcined for two hours at 400 °C. The absorption spectra revealed a broad band emission and a comparatively narrow absorption band at 360.68 nm, respectively.

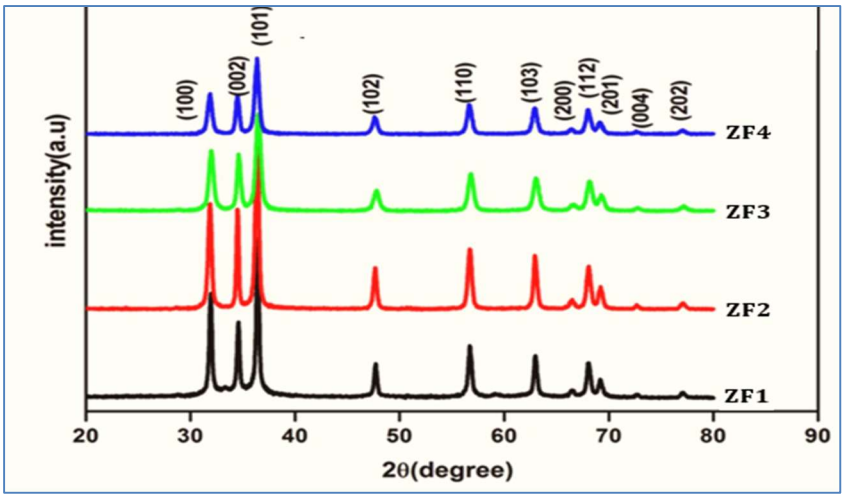

Fig. 1. XRD spectra of ZF1-ZF4

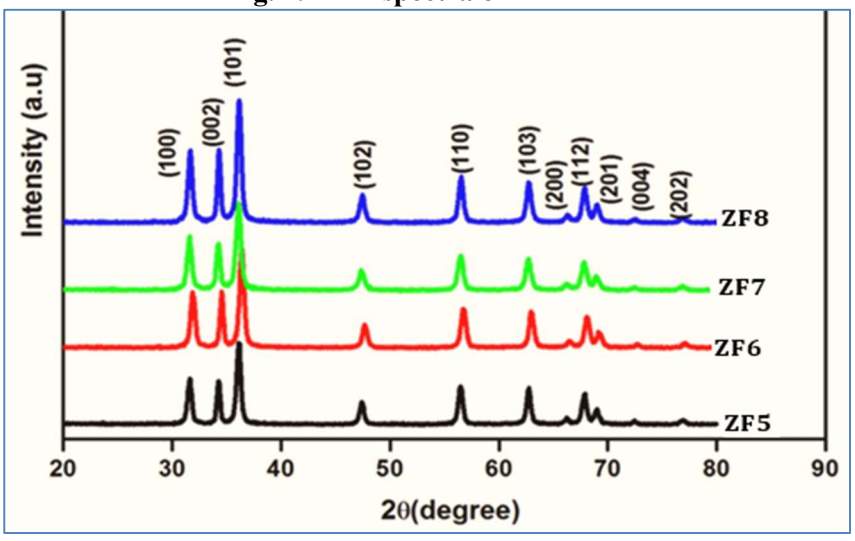

Fig. 2. XRD spectra of ZF5-ZF8

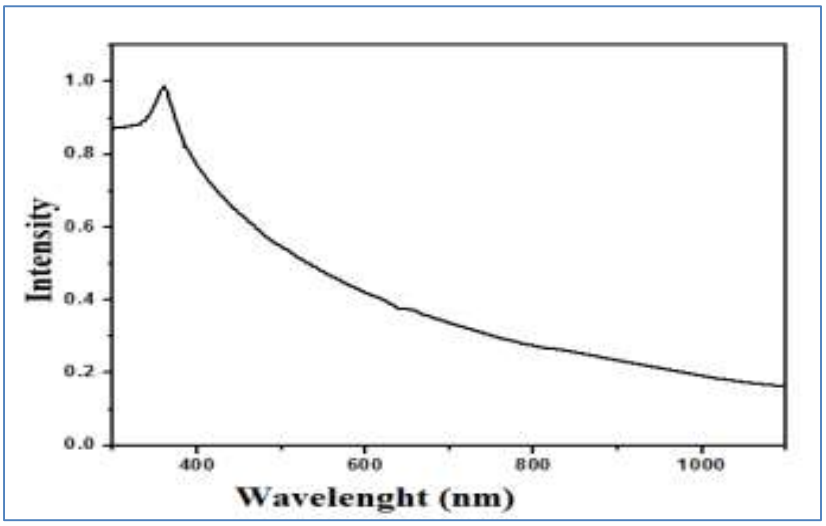

Figure 3: UV spectra of Prepared ZnO nanoparticles (ZF3)

Fourier Transform Infrared Spectroscopy (FT-IR) analysis: The FTIR spectra of ZnO nanoparticles synthesised in DEG and TEG is shown in Supplementary data Fig. 3. The characteristic peak at around 3437 cm−1 was ascribed to the stretching vibrations of the hydroxyl group, while the peaks at approximately 2925 cm−1 were assigned to the –CH stretching, indicating the existence of CH2,CH3 groups. Two peaks were attributed to symmetric and asymmetric C=O stretching, located at approximately 1595 cm−1 and 1383 cm−1, respectively. Peak location at 1118 cm−1 was attributed to –CH deformation, demonstrating bending of –CH2, and –CH3. Metal oxides typically display absorption bands in the fingerprint region below 1000 cm−1 as a result of interatomic vibrations. The peaks in the infrared spectrum at approximately 575 cm−1 are attributed to ZnO and demonstrate the stretching vibration of Zn–O. This observation indicate that, DEG/ TEG molecules get adsorbed on synthesized ZnO nanoparticles. The differences in the particle sizes may lead to different wavenumber and frequencies are consistent to the reported literature.

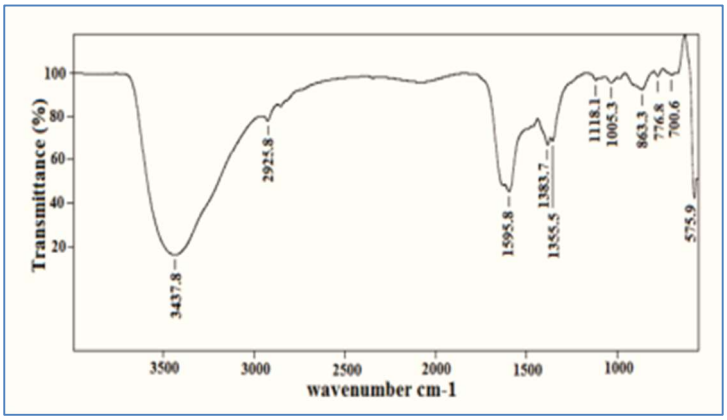

Figure 3: UV spectra of Prepared ZnO nanoparticles (ZF3)

Thermogravimetric analysis: Using TGA analysis, all ZnO samples' thermal breakdown behaviour and the existence of adsorbed polyols were noted. Every sample was heated at a rate of 10 °C per minute, from 50 to 900 °C. The thermal degradation of ZnO nanoparticles synthesised by TEG and DEG, respectively, is depicted in Supplementary Data Fig. 4. In every sample, the two subsequent decompositions were noted. The first stage of decomposition was caused by the evaporation of surface-adsorbed water and moisture, which happened in the range of 0–400 °C.

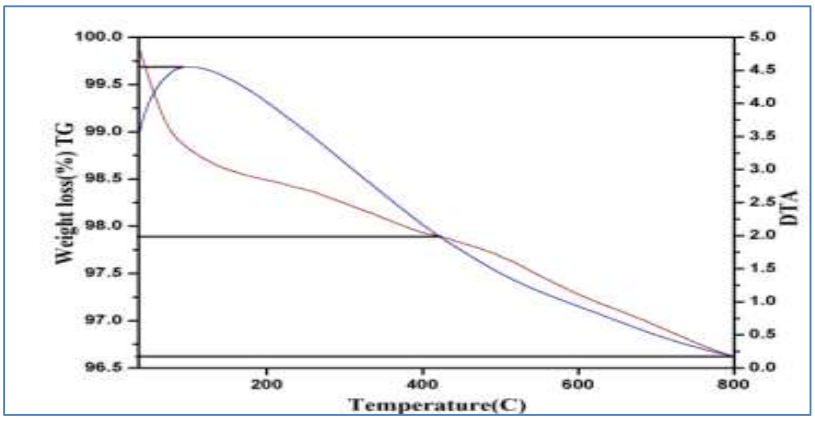

Figure 4: DSC of Prepared ZnO nanoparticles (ZF3 and ZF8)

SEM Analysis: SEM images of the ZnO nanoparticle prepared by chemical method. The SEM analysis has showed agglomeration of the particles and in the range of 10 µm. The TEM analysis particles size is 10nm.

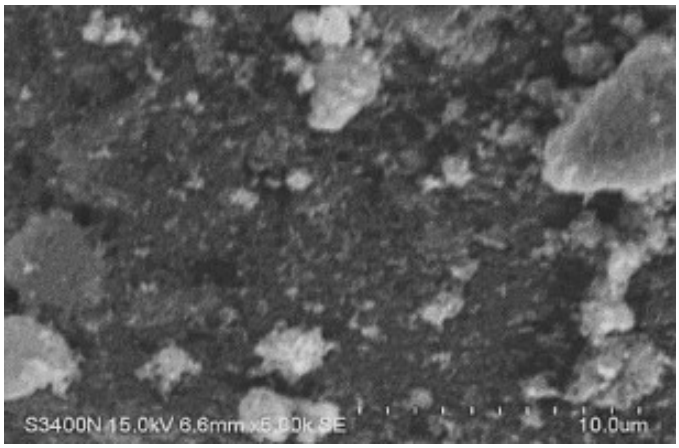

Figure 5: SEM of Prepared ZnO nanoparticles (ZF1)

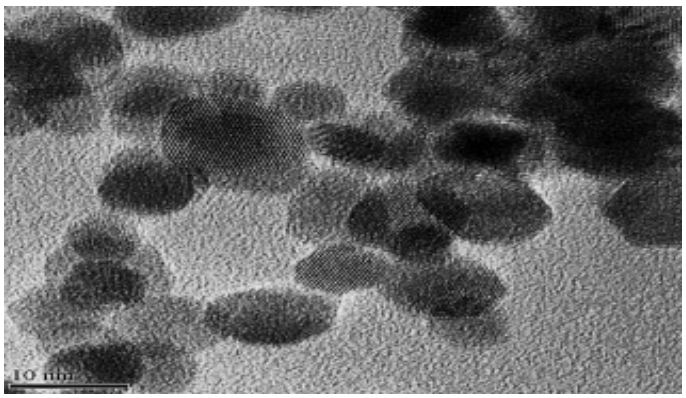

Figure 6: TEM of Prepared ZnO nanoparticles (ZF1)

Antibacterial study: Six clinically isolated strains of bacteria—Bacillus subtilis, Escherichia coli, Klebsiella pneumoniae, Pseudomonas aeruginosa, Salmonella typhi, and Staphylococcus aureus—were the subjects of an antibacterial investigation. Precursor zinc acetate dihydrate (0.1 M) was refluxed in diethylene glycol and triethylene glycol at 180 and 220 degrees Celsius, respectively, to create ZnO nanoparticles. Tables 2 and 3 display the zone of inhibition measurements for ZF1-ZF8.

The antibacterial activity of ZF1 and ZF7 is about equal, but that of the other particles was lower than that of the other samples. According to the early results of the antibacterial activity investigation, ZF3 and ZF8 exhibit the highest activity against gram-negative K. pneumoniae (17.56±0.74 and 17.32±0.54), while ZF4 and ZF7 exhibit the highest activity against gram-negative P. aeruginosa (15.23±0.21 and 15.65±0.14), respectively, when compared to the other five strains. Therefore, it can be said that zinc oxide nanoparticles have antibacterial action against a wide range of microorganisms, regardless of the production process used. While the exact mode of action of zinc oxide particles on bacteria is still being studied, it has been proposed that the inhibitory impact could be caused by electrostatic interactions between the surface of the bacterium and the nanoparticles. The presence of ZnO nanoparticles leads to damages to the membrane wall of the bacteria. Also, when particles are in the form of large agglomerates, they are less likely to penetrate through the cell wall and damage the bacteria from the interior.

Table 2: Zone of inhibition of ZF1-ZF4

Bacterial strains	Zone of Inhibition (in mm)				
	ZF1	ZF2	ZF3	ZF4	Std.
Escherichia coli	16.17±0.91	9.11±0.34	15.33±0.42	12.17±0.34	34.33±0.21
Bacillus subtilis	6.34±0.95	12.11±0.78	15.17±0.40	10.98±0.34	40.33±0.33
Pseudomonas aeruginosa	12.78±0.34	10.98±0.40	12.56±0.91	15.23±0.21	41.83±0.17
Klebsiella pneumoniae	8.99±0.54	15.17±0.32	17.56±0.74	13.56±0.95	38.67±0.21
Staphylococcus aureus	11.32±0.54	12.65±0.44	16.17±0.65	15.83±0.54	39.33±0.21
Salmonella typhi	15.87±0.95	10.45±0.21	12.76±0.32	15.54±0.12	40.17±0.17

The value of each constituents consisted of ±S.D. of 6 replicates, $p< 0.01$

Table 3: Zone of inhibition ZF5-ZF8

Bacterial strains	Zone of Inhibition (in mm)				
	ZF5	ZF6	ZF7	ZF8	Std.
Escherichia coli	8.65±0.34	15.98±0.46	15.43±0.11	16.19±0.65	34.33±0.21
Bacillus subtilis	11.56±0.95	10.98±0.43	14.56±0.46	15.11±0.54	40.33±0.33
Pseudomonas aeruginosa	9.65±0.34	14.11±0.40	15.65±0.14	12.67±0.17	41.83±0.17
Klebsiella pneumoniae	13.65±0.56	12.65±0.32	15.65±0.46	17.32±0.54	38.67±0.21
Staphylococcus aureus	14.32±0.32	12.65±0.54	15.17±0.55	17.83±0.43	39.33±0.21
Salmonella typhi	15.87±0.95	13.45±0.67	15.66±0.32	15.76±0.32	40.17±0.17

The value of each constituents consisted of ±S.D. of 6 replicates, $p< 0.01$

CONCLUSION

In the current study, ZnO nanoparticles were created using three distinct methods: i) routine synthesis in polyols, ii) in the presence of sodium acetate, and iii) lengthening the reaction time. We demonstrated how these methods can be used to regulate the size and form of nanoparticles. This study shown that ZnO nanoparticles become more effective against bacteria as their particle size decreases. We have shown that using various techniques influences the size and form of the nanoparticles; these results offer a deeper comprehension of ZnO nanoparticles that may have antibacterial properties.

REFERENCES

1. Davies J, Davies D. Origins and evolution of antibiotic resistance. Microbiol Mol Biol Rev (2010) 74(3):417–33. doi:10.1128/MMBR.00016-10
2. Cavalieri F, Tortora M, Stringaro A, Colone M, Baldassarri L. Nanomedicines for antimicrobial interventions. J Hosp Infect (2014) 88(4):183–90. doi:10.1016/ j.jhin.2014.09.009
3. Reygaert W. An overview of the antimicrobial resistance mechanisms of bacteria. J AIMS microbiology (2018) 4(3):482–501. doi:10.3934/microbiol.2018.3.482
4. Kumar A, Schweizer HP. Bacterial resistance to antibiotics: active efflux and reduced uptake. Adv Drug Deliv Rev (2005) 57(10):1486–513. doi:10.1016/j.addr.2005.04.004
5. Blair JM, Richmond GE, Piddock LJ. Multidrug efflux pumps in Gram-negative bacteria and their role in antibiotic resistance. Future Microbiol (2014) 9(10): 1165–77. doi:10.2217/fmb.14.66
6. Reygaert W. Methicillin-resistant Staphylococcus aureus (MRSA): molecular aspects of antimicrobial resistance and virulence. Clin Lab Sci (2009) 22(2): 115–9. doi:10.29074/ascls.22.2.115
7. Vishvakrama P, Sharma S. Liposomes: an overview. Journal of Drug Delivery and Therapeutics. 2014 Jun 24:47-55.
8. Vishvakarma P. Design and development of montelukast sodium fast dissolving films for better therapeutic efficacy. Journal of the Chilean Chemical Society. 2018 Jun;63(2):3988-93.
9. Vishvakarma P, Mandal S, Verma A. A review on current aspects of nutraceuticals and dietary supplements. International Journal of Pharma Professional's Research (IJPPR). 2023;14(1):78-91.
10. Prabhakar V, Agarwal S, Chauhan R, Sharma S. Fast dissolving tablets: an overview. International Journal of Pharmaceutical Sciences: Review and Research. 2012;16(1):17.
11. Mandal S, Vishvakarma P, Verma M, Alam MS, Agrawal A, Mishra A. Solanum Nigrum Linn: an analysis of the Medicinal properties of the plant. Journal of Pharmaceutical Negative Results. 2023 Jan 1:1595-600.
12. Vishvakarma P, Mandal S, Pandey J, Bhatt AK, Banerjee VB, Gupta JK. An Analysis of The Most Recent Trends in Flavoring Herbal Medicines in Today's Market. Journal of Pharmaceutical Negative Results. 2022 Dec 31:9189-98.
13. Langford B, So M, Raybardhan S, Leung V, Westwood D, MacFadden D, et al. Bacterial co-infection and secondary infection in patients with COVID-19: a living rapid review and meta-analysis. Clin Microbiol Infect (2020) 26(12): 1622–29. doi:10.1016/j.cmi.2020.07.016
14. Sharifipour E, Shams S, Esmkhani M, Khodadadi J, Fotouhi-Ardakani R, Koohpaei A, et al. Evaluation of bacterial co-infections of the respiratory tract in COVID-19 patients admitted to ICU. BMC Infect Dis (2020) 20(1):646. doi:10.1186/s12879-020-05374-z
15. Pholnaka C., Sirisathitkula C., Suwanboonb S., Hardinga D.J. Effects of precursor concentration and reaction time on sonochemically synthesized ZnO nanoparticles, Mater. Res. 2014; 17(2): 405-411.
16. Jung H.M., Chu M.J. Synthesis of hexagonal ZnOnanodrums, nanosheets and na- nowires by the ionic effect during the growth of hexagonal ZnO crystals, J. Mater. Chem. 2 (2014) 6675–6682.
17. Yasuyuki M, Kunihiro K, Kurissery S, Kanavillil N, Sato Y, Kikuchi Y Antibacterial properties of nine pure metals: a laboratory study using Staphylococcus aureus and Escherichia coli. Biofouling (2010) 26(7):851–8. doi:10.1080/08927014.2010.527000
18. Lemire JA, Harrison JJ, Turner RJ Antimicrobial activity of metals: mechanisms, molecular targets and applications. Nat Rev Microbiol (2013) 11(6):371–84. doi:10.1038/nrmicro3028
19. Hanley C, Layne J, Punnoose A (2008) Preferential killing of cancer cells and activated human T cells using zinc oxide nanoparticles. Nanotechnology 19:295103–13
20. Jones N, Ray B, Ranjit KT, Manna AC (2008) Antibacterial activity of ZnO nanoparticle suspensions on a broad spectrum of microorganisms, FEMS Microbiology Letters 279 :71–76
21. Maensiri S, Loakul P, Klinkaewnarong, Phokha S, Promarak V, Seraphin S (2008) Indium Oxide nanoparticles using Aloe vera plant extract:synthesis and optical properties, Journal of optioelectronics and advanced materials 10: 161-165

22. Makhluf S, Dror R, and Nitzan Y (2005) Microwave-assisted synthesis of nanocrystalline ZnO(MgO) and its use as bacteriocide 15: 1708-1715
23. Valko M, Morris H, Cronin MT Metals, toxicity and oxidative stress. Curr Med Chem (2005) 12(10):1161–208. doi:10.2174/0929867053764635
24. Li WR, Xie XB, Shi QS, Zeng HY, Ou-Yang YS, Chen YB Antibacterial activity and mechanism of silver nanoparticles on Escherichia coli. Appl Microbiol Biotechnol (2009) 85(4):1115–22. doi:10.1007/s00253-009-2159-5
25. Pereira Y, Lagniel G, Godat E, Baudouin-Cornu P, Junot C, Labarre J Chromate causes sulfur starvation in yeast. Toxicol Sci (2008) 106(2): 400–12. doi:10.1093/toxsci/kfn193
26. Maret W Metals on the move: zinc ions in cellular regulation and in the coordination dynamics of zinc proteins. Biometals (2011) 24(3):411–8. doi:10. 1007/s10534-010-9406-1
27. Shakibaie M., Forootanfar H., Golkari Y., MohammadiKhorsand T., Shakibaie M. Anti-biofilm activity of biogenic selenium nanoparticles and selenium dioXide against clinical isolates of Staphylococcus aureus, Pseudomonas aeruginosa, and Proteus mirabilis, J. Trace Elem. Med. Biol. 29 (2015) 235–241.
28. Ashajyothi C., Manjunath R., Chandrakanth R. Prevention of multiple drug re- sistant bacterial biofilm by synergistic action ofbiogenic silver nanoparticle and antimicrobials, J. Microbiol Biotechnol. Res. 5 (1) (2015) 14–21.
29. Gutierrez M.F., Boegli L., Agostinho A., Sánchez M.E., Horacio B., Ruiz F., James G. Anti-biofilm activity of silver nanoparticles against different microorganisms, Biofouling 29 (6) (2013) 651–660.
30. Applerot G., Lellouche J., Perkas N., Nitzan Y., Gedanken A., Banin E. ZnO nano- particle-coated surfaces inhibit bacterial biofilm formation and increase antibiotic susceptibility, RSC Adv. 2 (2012) 2314–2321.
31. Ashajyothi C., Handral Harish V., Dubey N., Chandrakanth R. Antibiofilm activity of biogenic copper and zinc oXide nanoparticles-antimicrobials collegiate against multiple drug resistant bacteria: a nanoscale approach, J. Nanostruct. Chem. 6 (2016) 329–341.
32. Lee K.H., Park S.J., Choi S.J., Park J.Y. Proteus vulgaris and Proteus mirabilis de- crease Candida albicans biofilm formation by suppressing morphological transition to its hyphal form, J. YMJ 58 (2017) 6,1135.
33. Darouiche R.O. Treatment of infections associated with surgical implants, N. Engl. J. Med. 350 (2004) 1422–1429.
34. David R.H., Parracho M.R.T.H., Walker J., Sharp R., Hughes G., Werthén M., Lehman S., Morales S. Bacteriophages and biofilms, Antibiotics 3 (2014) 270–284.
35. Mollica A., Macedonio G., Stefanucci A., Costante R., Carradori S., Cataldi V., Di Giulio M., Cellini L., Silvestri R., Giordano C., Scipioni A., Morosetti S., Punzi P., Mirzaie S. Arginine- and lysine-rich peptides: synthesis, characterization and antimicrobial activity, Lett. Drug Des. Discov. 14 (2017) 1–7.